

# OPTICS DESIGN CONSIDERATIONS FOR THE CLIC PRE-DAMPING RINGS

F. Antoniou, National Technical University of Athens, Greece  
 Y. Papaphilippou, CERN, Geneva, Switzerland

## Abstract

The CLIC pre-damping rings have to accommodate a large emittance beam, coming in particular from the positron source and reduce its size to low enough values for injection into the main damping rings. Linear lattice design options based on an analytical approach for theoretical minimum emittance cells are presented. In particular the parameterisation of the quadrupole strengths and optics functions with respect to the emittance and drift lengths is derived. Complementary considerations regarding constraints imposed by positron stacking and input momentum spread are also considered.

## CLIC PRE-DAMPING RINGS

The pre-damping rings (PDR) are an essential part of the CLIC injector complex, as they have to digest a 2.424 GeV beam with a large input normalized emittance and damp it down to a few  $\mu\text{m}$  emittance for injection to the damping rings (DR) [1]. The required input and output parameters for the PDR are presented in Table 1. Without the positron ring, the injected normalized emittance of a few mm coming directly from the source will not fit in the DR. Other limitations are the large positron momentum spread of around 1 % which necessitates a large momentum acceptance in the PDR and for the polarized positron option, stacking needs a long time to fill the ring with the required number of positrons per bunch [2]. The electron emittance, although 3 orders of magnitudes lower, is still 2 orders of magnitude higher than the required DR input emittance and 5 orders of magnitude higher than the extracted emittance of around 4 nm. An electron beam from the low energy linac injected directly to the DR may not encounter aperture restrictions. On the other hand, without an electron PDR and considering the damping time of around 1.5 ms in the DR, the large linac emittance will need at least 16.5 ms to reach equilibrium (without the effect of IBS), reaching almost the repetition time of 20 ms. In this respect, both electron and positron PDR are necessary.

## ANALYTICAL APPROACH FOR MINIMUM EMITTANCE CELLS

The Theoretical Minimum Emittance (TME) cell may be a good structure for the design of the PDR lattice. The TME condition is achieved, if the horizontal  $\beta$  and the dispersion  $\eta$  have a minimum in the center of the bending magnet and are equal to  $\beta_{cd} = \frac{L_d}{2\sqrt{15}}$ ,  $\eta_{cd} = \frac{\theta L_d}{24}$  where  $L_d$  is the length of the bending magnet and  $\theta = \frac{L_d}{\rho} = \frac{2\pi}{N}$  the bending angle, for  $N$  bends in the ring. The nor-

Table 1: CLIC PDR required injected and extracted parameters.

Parameters	injected		extracted
	$e^-$	$e^+$	
Bunch population [ $10^9$ ]	4.7	6.4	4.5
Bunch length [mm]	1	5	10
Energy Spread [%]	0.07	1.	0.5
Long. emittance [keV.m]	1.7	240	121
Hor. Norm. emittance [ $\mu\text{m}$ ]	100	$9.7 \times 10^3$	63
Ver. Norm. emittance [ $\mu\text{m}$ ]	100	$9.7 \times 10^3$	1.5

malized TME is then given by  $\epsilon_{\text{TME}} = FC_q\gamma^3\theta^3$  where  $C_q = 3.84 \times 10^{-3}$  m. The scaling factor  $F$  for the TME lattice is  $F = \frac{1}{12\sqrt{15}J_x}$  and the damping partition number  $J_x \approx 1$ , in the case of isomagnetic, separated function dipoles [3]. In this respect, a minimum of  $N = 18$  dipoles with bending angle of  $20^\circ$  are needed  $\theta = \frac{2\pi}{N}$ , to achieve the required normalized emittance, taking a 30 % margin from the absolute minimum emittance of the TME cell (i.e. 41  $\mu\text{m}$ ).

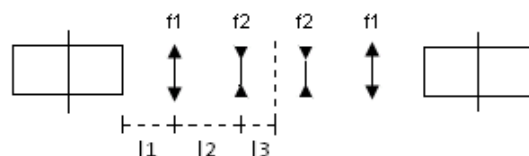


Figure 1: Schematic view of a TME cell.

A schematic view of a TME cell is displayed in Fig. 1. At the entrance of the cell (i.e. the middle of the dipole), two independent optics constraints are imposed by the conditions for minimum emittance, and thus at least two quadrupole families are needed to achieve them. Whereas the horizontal optics functions are fully controlled by these two pairs of quadrupoles, the vertical are defined by the horizontal plane's constraints. In order to have an independent matching of the vertical plane, additional quadrupoles are needed. The problem may be solved analytically using thin lens approximation in order to parameterise the solutions with respect to the drift lengths (for constant emittance) or the emittance (for constant drift lengths). The general solutions for the focusing strengths  $f_1 = (K_1l)^{-1}$  and  $f_2 = (K_2l)^{-1}$  are:

$$\begin{aligned} f_1 &= \frac{L_d^2 - 8(l_1 + l_2)L_d(\eta_{cd} - \rho) + 16(\eta_{cd} - \eta_s)\rho^2}{l_2(L_d^2 + 16\eta_{cd}\rho^2) + 8l_1L_d(\rho - \eta_{cd})} \\ f_2 &= \frac{-L_d^2 + 8l_1L_d(\eta_{cd} - \rho) + 16(\eta_s - \eta_{cd})\rho^2}{16l_2\eta_s\rho^2} \end{aligned} \quad (1)$$

where  $\eta_s$  is the dispersion function at the center of the cell, which has a complicated dependence on the drift lengths, the initial optics functions and the bending characteristics. There are two solutions for  $\eta_s$  but one results in focal lengths of the same sign (horizontally focusing quadrupoles) and can be rejected as it leads to an unstable vertical plane.

For stability in both planes, as well as reasonable optics functions, the following conditions have to be satisfied:

- $\text{Trace}(M_{x,y}) = 2 \cos \mu_{x,y} < 2$ , where  $M_{x,y}$  is the total transfer matrix of the cell and  $\mu_{x,y}$  are the phase advances per cell.
- $f_1 f_2 < 0$
- All the optics functions have real values in all the elements of the cell.
- The beta function maxima should be below 30 m.

All the optics functions are thus uniquely determined for both planes and can be optimized by varying the drifts.

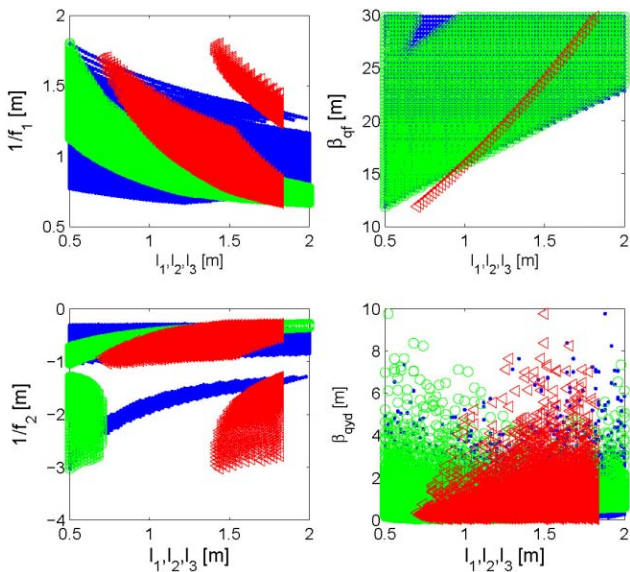


Figure 2: Focusing strengths (left) and maximum beta functions (right) dependence on the drift lengths. The red triangles represent the dependence on  $l_1$ , the green circles on  $l_2$  and the blue dots on  $l_3$ .

We consider, first, a constant emittance (the minimum one) and seek for the regions of acceptable solutions for the drift lengths and the focusing strengths. Figure 2 shows the dependence on the drift lengths, of the focusing strengths  $f_1, f_2$ , the horizontal  $\beta_{x,f_1}$  and vertical  $\beta_{y,f_2}$  beta functions on each quadrupole, where they take their maximum values. The red triangles denote the dependence of the functions on  $l_1$ , the green circles on  $l_2$  and the blue dots on  $l_3$ . All three drift lengths are set to vary between 0.5 and 2 m. The plots show that there is no restriction for  $l_2$  and  $l_3$ , whereas the values of  $l_1$  are bounded between 0.7 and 1.82 m. The upper limit is set by the maximum beta function requirement and the lower by the requirement for real solutions. The focusing strengths is scaled inversely to  $l_1$  and

$l_2$  but there is no clear tendency for the dependence on  $l_3$ . The horizontal beta function on the focusing quadrupole presents the usual quadratic dependence on the first drift length  $l_1$ , but there is no dependence on the downstream drifts, apart from the delimitation in the bottom left corner due to the stability requirement. The dependence of the vertical beta function on the drift lengths is less obvious. It is interesting though that the maximum beta function is below 10 m for the range of drift lengths considered.

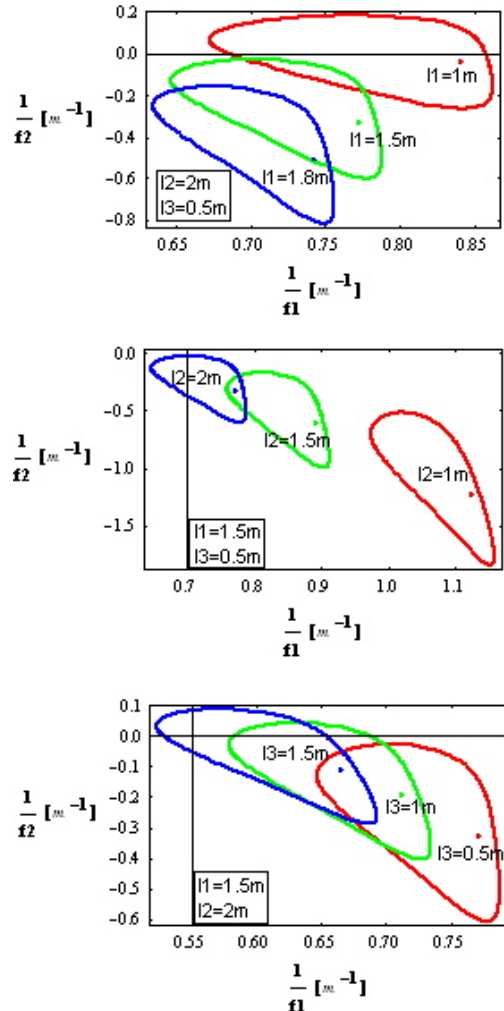


Figure 3: Emittance dependence on each drift length. From top to bottom, one of the drifts takes three distinct values whereas the other two are kept constant.

In Fig. 3, the dependence of the focusing strength on the emittance is presented, using the drifts as parameters. From the top to the bottom plot, one of the drifts takes three distinct values whereas the other two are kept constant. The emittance required is the TME one and twice this value. For the TME, there are unique values in the quadrupole strengths displayed by dots in the plots, as shown by equation (1). The relaxed emittance can be achieved by a series of  $(\eta_{cd}, \beta_{cd})$  pairs, with a quadratic dependence to each other. In this respect, these solutions will appear as dis-

torted ellipses in the focusing strength plane. From the top plot, one can conclude that by decreasing  $l_1$ , the focusing strength of the first quadrupole is only slightly increased whereas there is a big impact in the reduction of the second quadrupole strength. The dependence on  $l_2$  and  $l_3$  is the same for both quadrupoles, i.e. longer drifts reduce their strength. Combining the information from the above, a good choice for drift values are  $l_1 = 1.5$  m,  $l_2 = 2$  m and  $l_3 = 0.5$  m, in order to achieve reasonable strengths and optics parameters for the TME cell.

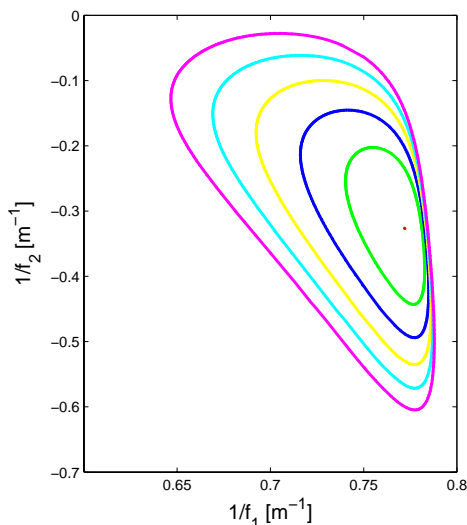


Figure 4: The focusing strengths parameterised with different emittance values. Each curve with different colors corresponds to a certain emittance value, starting from the TME (red dot) up to 2 times the TME (purple).

For these drift lengths, eqs. (1) are solved for different emittances, ranging from the TME up to 2 times this value with a 0.2 step. The parameterisation of the focusing strengths with the emittance is displayed in Fig. 4. It is not a surprise that larger emittances can be reached by a wider range of focusing strengths. This plot solves completely the problem of matching the optics for TME cells, and it can be used for other optics parameters' optimization, such as aperture, phase advances, chromaticity, sextupole strengths, momentum compaction, etc.

Figure 5 shows the dependence of several other radiation parameters on the bending field. A fixed cell achieving the TME is considered and the bending field is varied by changing the dipole length, while keeping the bending angle constant. The dependence of the momentum compaction factor  $\alpha_c$ , is inversely proportional to the bending field but still of the order of a few  $10^{-3}$ , ten times bigger than the one of the DR. This is due to the fact that, for achieving a TME, the momentum compaction is  $\alpha_c = \frac{12\theta^3 \rho}{C}$ , i.e. proportional to the bending radius for fixed bending angle. In order to increase the momentum acceptance to the  $\pm 1\%$  level, the momentum compaction

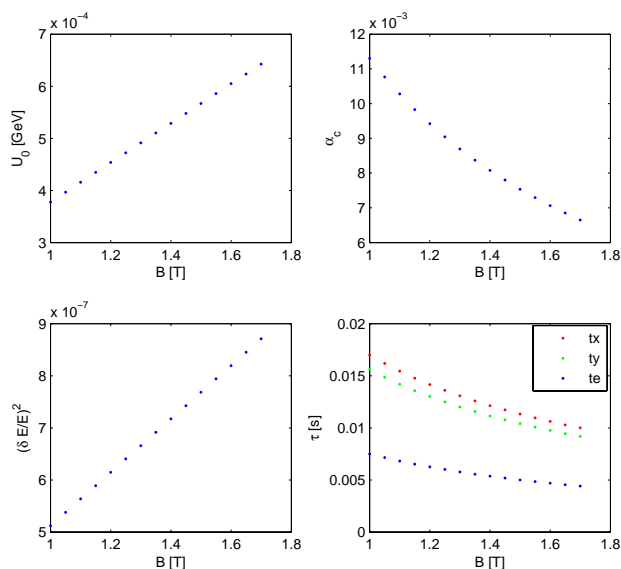


Figure 5: Dependence on the bending field, for a TME cell, of the energy loss per turn (top left), square of the rms energy spread (bottom left), momentum compaction (top right) and damping times (bottom right).

factor has to be further reduced, by decreasing the bending angle (larger number of cells) and by detuning the lattice to a higher emittance, and imposing negative dispersion in the center of the dipole. The energy acceptance can be increased by raising the RF voltage or using harmonic cavities.

The damping partition number  $D$  for a TME is a constant depending only on the bending angle  $D = \frac{12\theta^3}{2\pi}$ , and equal to around  $10^{-1}$  for the chosen parameters. This makes  $J_x$  slightly less than 1, which is also reflected in the few % difference between the horizontal and vertical damping times. These later are around 13-14 ms, quite long and ten times higher than the ones in the DR. They are indeed incompatible with the long stacking time of 12 ms necessary for filling the positron ring, with a repetition time of 20 ms. In order to achieve fast damping times of around 0.8 ms (i.e. twice faster than in the DR), damping wigglers may not be enough. An interleaved train injection scheme should be considered for the positron ring, with at least 4 trains, considering normal conducting wigglers of the same length, as the one of the DR. In this respect the lattice design is not the only challenge but also the handling of high beam power, the design of HOM free RF cavities and impact of other collective effects.

## REFERENCES

- [1] Y. Papaphilippou, *et al.*, these proceedings.
- [2] F. Tecker (ed.) *et al.*, CLIC note 764, to be published.
- [3] S.Y. Lee, Accelerator Physics, World Scientific, 2004.
- [4] R. Talman, "Converting an  $e^+/e^-$  collider into a bright X-ray source", unpublished.